Hindawi
Advances in Materials Science and Engineering
Volume 2022, Article ID 3539069, 9 pages
https://doi.org/10.1155/2022/3539069

Research Article

A Novel Approach to the Sintering Schedule of Ba (Co0.7Zn0.3)1/3Nb2/3O3 Dielectric Ceramics for Microwave Applications

Mohamed Mouyane, Brahim Itaalit, Jérôme Bernard, and David Houivet

Laboratoire Universitaire des Sciences Appliquées de Cherbourg (LUSAC), Normandie Univ, UNICAEN, LUSAC, EA 4253, France

Correspondence should be addressed to Mohamed Mouyane; mohamed.mouyane@unicaen.fr

Received 8 March 2022; Revised 9 May 2022; Accepted 24 May 2022; Published 22 July 2022

Academic Editor: Ravi Samikannu

The present research is devoted to the optimization of the sintering schedule of Ba (Co0.7Zn0.3)1/3Nb2/3O3 (BCZN) dielectric ceramics for microwaves applications. A novel approach to the heat treatment of these ceramics based on the rapid-rate sintering (RRS) technique followed by a lower temperature annealing cycle has been developed. The relationships among the heat treatment process optimization, the structural, microstructural characteristics, and the microwave dielectric properties of the BCZN ceramics were investigated using X-ray diffraction, scanning electron microscopy, energy dispersion analysis, and vector network analysis. The RRS-technique shortens substantially the time required for the elaboration of these components in comparison with conventional sintering techniques and prevents simultaneously the formation of secondary phases as Ba5Nb4O15 and Ba8(Co, Zn) 1Nb6O24 on the surface of the ceramics. All of the sintered and annealed ceramics exhibit a high quality factor QF close to 110 000 GHz at 6 GHz. The high dielectric constant εr of ~34.5 and a temperature coefficient of the resonant frequency τf of ~0 ppm.C-1 were obtained in all annealed ceramics.

1. Introduction

In particular, Ba (Co0.7Zn0.3) 1/3Nb2/3O3 (BCZN) is one of the main compounds studied nowadays as a ceramic resonator in microwave applications and as a cheap alternative to Ta-based complex perovskite ceramics such as BaZn1/3Ta2/3O3 (BZT), which have a great commercial success [1]. In Ba (Co0.7Zn0.3)1/3Nb2/3O3, barium as the larger cation occupies the A-sites, while Co, Zn, and Nb are found on B-sites. Ba (Co0.7Zn0.3)1/3Nb2/3O3 shows a typical Ba (B′1/3B″2/3)O3 perovskite structure where B′ is a mixture of Co and Zn atoms and B″ is a Nb atom. The structure is characterised by a 1:2 arrangement of Co, Zn (B′), and Nb (B″) atomic columns [2]. This 1: 2 cation ordering, which is obtained only by heat treatments at high temperatures, has been shown to be the essential property responsible for the interesting electric properties of this material [3], such as a high quality factor QF (low dielectric loss), a high dielectric constant $\varepsilon r = 34.5$, and a near zero temperature coefficient of the resonant frequency τf [4, 5]. In particular, the QF-factor value is strongly affected by the degree of cation ordering. Recently, it has been reported that the disordered BCZN ceramic has a low value of QF (12 000 to 36 000 GHz at 6 GHz), whereas the ordered BCZN ceramic exhibits a higher QF value up to 123 700 GHz [2, 6]. In dense BCZN ceramic materials, this kind of ordering is difficult to accomplish without the use of additional procedures such as adding impurities [7–9] or the use of a second thermal treatment as an annealing process [2, 3, 6]. In the case of BCZN, an ordered structure was obtained by an annealing process at 1300°C for 12 h [6]. In our previous work [3, 6], we proved that the improvement of the quality factor QF of such ceramic materials is related to the 1:2 cation ordering in the BCZN crystal that occurs during the annealing process. By adding an annealing step as a second thermal treatment following the initial sintering step, we obtained BCZN materials with excellent dielectric properties ($\varepsilon r = 34.5$, QF= 123 700 GHz, and $\tau f = 0$ ppm/°C). However,

the total time required to obtain this result was quite long, 16.25 hours for the sintering step plus 30 hours for the annealing process [6]. As a continuation of our previous work, the present paper describes a novel approach to the sintering of BCZN ceramics by using the rapid-rate sintering (RRS) technique. The comparisons between the present and previous works [3, 6] have been explored to highlight the advantages of the RRS-technique compared to sintering and postsintered annealing of BCZN ceramics. This technique has been largely employed for the synthesis of ceramic materials in order to improve their densification and to avoid undesired grain growth [10–14]. However, the use of the RRS-technique has not yet been reported in the literature for the synthesis of BCZN ceramics. Kim et al. [14] believe that the use of the RRS-technique for sintering indium tin oxide (ITO) could be beneficial to prevent evaporation of ITO material. In the case of BCZN ceramics, it could be expected that the RRS concept allows to obtain dense BCZN materials and to avoid simultaneously the evaporation of cobalt and zinc atoms during the sintering process, preventing in this way the formation of secondary surface phases such as Ba5Nb4O15 and Ba8 (Co, Zn) 1Nb6O24 as they were observed in our previous study [6].

The aim of the present work was thus to produce dense BCZN ceramic materials in a shorter time by simultaneously limiting the formation of undesired surface phases.

2. Experimental Section

The Ba (Co0.7Zn0.3) 1/3Nb2/3O3 (BCZN) ceramics were prepared using the aqueous mixing technique-assisted solid-state method as described previously [3]. Oxides (Co_3O_4, Nb_2O_5, and ZnO) and carbonate precursors (BaCO3) with high purity (≥99%) are used as the raw material. The dried powders were calcined in the air at 1000°C for 2 h in an electric furnace. The BCZN powders were formed into cylindrical pellets of about 10 mm in diameter and 5 mm height by uniaxial pressing with a pressure of 200 MPa. The rapid-rate sintering technique was achieved by placing the pellets in an alumina boat, which was then introduced into a tubular furnace by using a horizontal alumina push rod which moved the sample from the cold to the hot zone of the furnace at a constant speed. An alumina tube with an inside diameter of 6 cm and a length of 150 cm is used. The homogeneous heating zone is 15 cm. The sintering treatment was carried out in an atmosphere of air. The insertion and extraction speed as well as the sintering temperature were controlled by an automated system. The sintering temperature was fixed at 1450°C under air. The insertion/extraction times ranged between 5 and 100 minutes (100 minutes is equivalent to a heating or cooling rate equal to 858°C h^{-1}), and the holding time ranged between 0 and 60 minutes. The illustrative scheme of the RRS equipment is shown in Figure 1. Five samples were sintered under different thermal conditions. These ceramics are called x1s, x2s, x3s, x4s, and x5s. They were then annealed at 1300°C for 30 h in air which gave respectively the so-called samples x1a, x2a, x3a, x4a, and x5a. (The "s" and "a" letters correspond respectively to sintered and annealed samples). The sintering parameters are presented in Table 1. The heating and cooling rates of the annealing process were 200°C h^{-1}. A Siemens D5005 X-ray diffractometer using CuKα radiation (λ= 1.540562 Å) was used to identify surface and bulk crystalline phases in the sintered and annealed ceramics. Diffractograms were recorded in the continuous mode for 2θ angles ranging from 15 to 60°. The X'pert High Score program was used for phase matching. A microstructural observation of the ceramics was performed with a scanning electron microscope (SEM, Hitachi S3400) combined with an energy dispersive spectrometer (EDS, ThermoNoran). The SEM micrographs were collected on the polished and unpolished surfaces. In this context, surfaces of the ceramics were polished successively using various grades of silicon carbide papers, and 1.0 μm diamond paste was used for the final polishing. The polished pellets were treated thermally at 1100°C for 20 minutes to reveal grain boundaries. In addition, the experimental densities of the unpolished sintered pellets were measured with a Micromiritics AccuPyc 1330 helium pycnometer and compared to the geometrical densities of the corresponding samples. The open porosity was derived from the relation between the skeleton and the geometrical densities. The results of BCZN ceramic densities are gathered in Table 2. Finally, the dielectric properties were measured at 6 GHz resonance frequency on the unpolished sintered pellet using an Agilent 8722ES vector network analyzer, and the results are gathered in Table 3.

3. Results and Discussion

3.1. Structural and Microstructural Observations. Figures 2(a) and 2(b) show X-ray diffraction patterns recorded on the surface of the Ba (Co0.7Zn0.3) 1/3Nb2/3O3 (BCZN) ceramics after sintering at 1450°C (samples x1s to x5s) and after annealing at 1300°C for 30 h (samples x1a to x5a). All diffraction peaks of the sintered BCZN ceramics (Figure 2(a)) can be indexed using the structure of BaZn1/3Nb2/3O3 ceramics (JCPDS card No. 39–1474), a cubic perovskite structure with space group Pm3m, indicating that the cosubstitution for Zn atoms does not affect the structure with just a very slight diminution of the cubic cell volume. Only some tiny peaks have not been identified. This result suggests that the as-prepared specimens are not affected by the thermal cycle used for the sintering step (RRS technique). Thus, the rapid-rate sintering technique permits to produce pure BCZN ceramics by avoiding the formation of secondary phases such as Ba5Nb4O15 and Ba8 (Co, Zn) 1Nb6O24 on the surface of the BCZN specimens as they were observed in our previous work [3, 6] after sintering at 1450°C with slower heating/cooling rates (200°C h^{-1}) and a longer dwell time (2 hours). The XRD pattern of the BCZN annealed ceramics at 1300°C for 30 h in air are presented in Figure 2(b). The annealing process leads for all samples (x1a to x5a) to a mixture of three phases Ba (Co0.7Zn0.3)1/3Nb2/3O3 (BaZn1/3Nb1/6O3; JCPDS card No. 39–1474), Ba5Nb4O15 (JCPDS file 14–0028), and Ba8 (Co, Zn) 1Nb6O24 (JCPDS card 89–0693 which is the File N°. Of Ba8Ta6NiO24). The structure of Ba8Ta6NiO24 is used for indexing the Ba8 (Co, Zn) 1Nb6O24 peaks due to

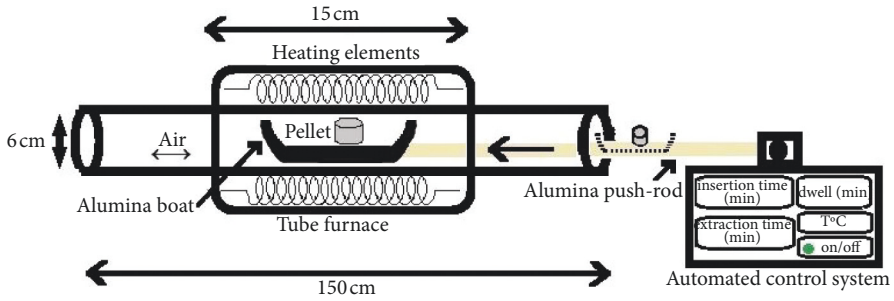

Figure 1: Schematic illustration of the rapid-rate sintering equipment.

Table 1: Sintering and annealing parameters of BCZN ceramics. Larger grain sizes are extracted from bulk samples (Figures 5(a) and 5(b)).

	Sintering parameters at 1450°C						Heating parameters at 1300°C			
Sample	Insertion time (min)	Dwell time (min)	Extraction time (min)	Sintering process time (min)	Larger grain size (μm)	Sample	Heating rate (°C/h)	Dwell time (h)	Cooling rate (°C/h)	Larger grain size (μm)
x1s	5	0	5	10	~2	x1a	200	30	200	~2
x2s	5	10	5	20	~4	x2a				~5
x3s	10	10	10	30	~5	x3a				~6
x4s	100	30	100	230	~7	x4a				~9
x5s	100	60	100	260	~10	x5a				~10

Table 2: Characteristic properties of annealed BCZN ceramics.

Sample	Sintering parameters at 1450°C Insertion-dwell-extraction times (min)	Density (g/cm3)		Porosity (%)			Shrinkage Δl/l (%)
		Geometrical	Skeleton	Total	Closed	Open	
x1a	5-0-5	6.29	6.37	3.23	2	1.23	15.92
x2a	5-10-5	6.23	6.29	4.15	3.23	0.92	16.41
x3a	10-10-10	6.21	6.3	4.46	3.08	1.38	16.55
x4a	100-30-100	6.22	6.33	4.31	2.62	1.69	16.43
x5a	100-60-100	6.22	6.32	4.31	2.77	1.54	16.62

Table 3: Dielectric properties (measured at 6 GHz) of sintered and annealed BCZN ceramics.

Sintering parameters at 1450°C Insertion-dwell-extraction times (min)	Sintered sample	QF (GHz) After sintering (1450°C)	Annealed sample	QF (GHz) After annealing (1300°C-30 h)
5-0-5	x1s	31 830	x1a	88653
5-10-5	x2s	40 699	x2a	112 598
10-10-10	x3s	40 888	x3a	109 594
100-30-100	x4s	48 003	x4a	107 964
100-60-100	x5s	52 799	x5a	107 491

isostructurality of these two compositions [15]. The intense peak at $2\theta = 37.93^{\circ}$ shows that the Ba8 (Co, Zn) 1Nb6O24 phase is majority on the BCZN surface ceramics. This result is in accordance with the previous works [7].

Figures 3(a) and 3(b) show X-ray diffraction patterns of the bulk of Ba (Co0.7Zn0.3) 1/3Nb2/3O3 (BCZN) ceramics after rapid-rate sintering at 1450°C with different thermal cycles (samples x1s to x5s) and after annealing at 1300°C for 30 h (samples x1a to x5a). As shown in Figures 3(a) and 3(b), all peaks can be indexed to the cubic structure of Ba(Co0.7Zn0.3)1/3Nb2/3O3 (BaZn1/3Nb1/6O3; JCPDS card No. 39-1474) together with the unidentified peak at 2 = 20° (particularly for x4a sample). Furthermore, for both thermal processes, namely, sintering (RRS technique) or annealing, it was noted that the secondary phases Ba5Nb4O15 and Ba8 (Co, Zn) 1Nb6O24 are not detected in the bulk materials. Ba5Nb4O15 and Ba8 (Co, Zn) 1Nb6O24 secondary phases are thus only present on the surface of the BCZN annealed ceramics. As stated in ref [16], the presence of Ba5Nb4O15 and Ba8 (Co, Zn) 1Nb6O24 phases on the BCZN surface ceramics during the annealing process was mainly due to a deficiency of some zinc and cobalt, which can be attributed to volatilization occurring during the long time the ceramics stayed at high temperature.

Figures 4(a) and 4(b) show the SEM micrographs of the surfaces of the BCZN ceramics after the RRS technique at 1450°C (samples x1s to x5s) and after the annealing process

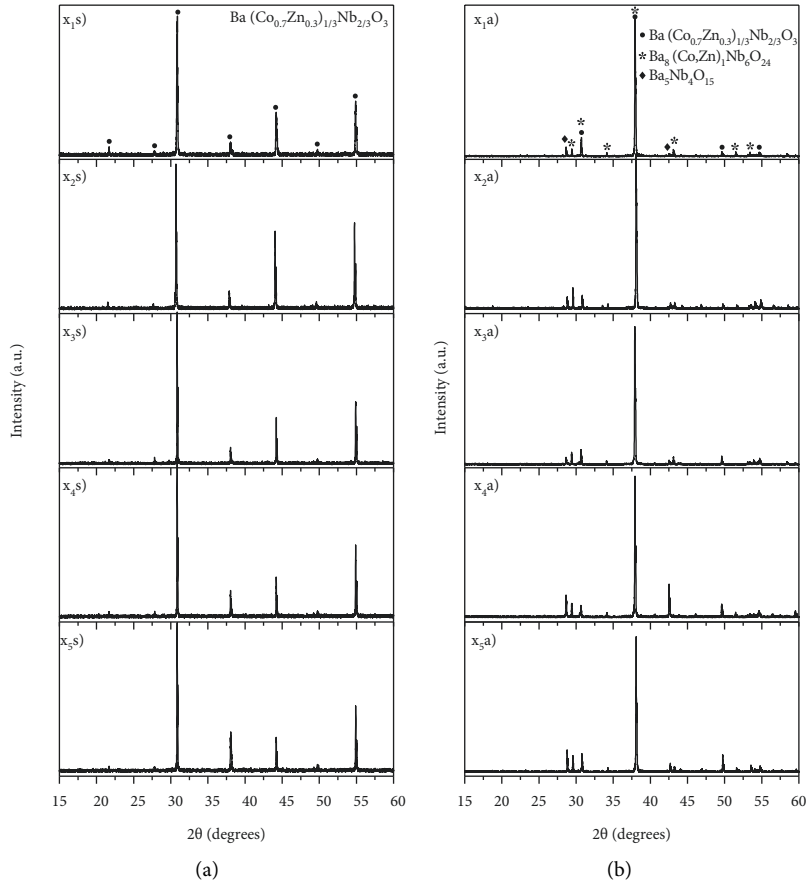

Figure 2: X-ray diffraction pattern taken from the surface of BCZN ceramics: (a) BCZN sintered ceramics recorded for different thermal cycles and (b) BCZN annealed ceramics at 1300°C for 30 (h) •: Ba (Co0.7Zn0.3) 1/3Nb2/3O3, *: Ba8 (Co, Zn) 1Nb6O24, and ◆: Ba5Nb4O15.

at 1300°C (samples x1a to x5a). The RRS-ceramics surfaces are formed of round shaped grains (Figure 4(a)). The grains size increase with the global sintering time (the samples from x1s to x5s are arranged in ascending order of dwell time at 1450°C as is reported in Table 1). On the other hand, we can also note that the larger grains of about 7 μm are observed in x5s-ceramic which corresponds to the insertion/extraction times of 100/100 minutes and a longer holding time of 60 min during the sintering process. Furthermore, the x1s-sample with zero dwell time and insertion/extraction times of 5/5 minutes exhibits the smallest values of the grain size (~1 μm).

The surface microstructures of BCZN ceramics annealed at 1300°C for 30 h are shown in Figure 4(b). The annealing process highlights the development of the secondary phases on the surface of the BCZN specimens with needle-shaped grains. This result is in accordance with that obtained from XRD analysis (see Figure 2(b)). The atomic percentages derived from the EDS spectra (not shown here) clearly revealed that the round particles consist of Ba (Co0.7Zn0.3) 1/3Nb2/3O3 composition, and the needle-shaped grains consist of the Ba8(Co, Zn) 1Nb6O24 phase, in good agreement with the XRD analyses (Figures 2(a) and 2(b)). These results are also in agreement with the literature [3, 7]. Figures 5(a) and 5(b) show the SEM images of the bulk BCZN ceramics after the RRS process at 1450°C (samples x1s to x5s) and after annealing process at 1300°C for 30 h (samples x1a to x5a). The SEM micrographs of BCZN bulk ceramics were taken from a depth of about 120 μm. The microstructure morphology observed for BCZN bulk sintered ceramics (Figure 5(a)) is similar with a round particle morphology observed of BCZN surface sintered ceramics (Figure 4(a)). However, increasing grain sizes were observed with the increasing sintering time process, with a larger typical grain size of 3–10 microns that has been observed in the x5s-sample (Figure 5(a)). This result is in accordance with the SEM analysis obtained on the sintered surface of BCZN specimens (Figure 4(a)). From Figure 5(b), it can be seen that the annealing process leads to similar morphologies as those observed for not annealed ceramics. These results are also in agreement with the XRD analyses (Figure 3(b)). On the basis of these experiments, we conclude that the annealing step at 1300°C for 30 h has a little effect on the grain growth (see Table 1). In contrast, secondary phase formation is developed. Table 2 shows the structural properties of the final annealed BCZN ceramics. The total porosity was calculated by the difference between the geometrical and the theoretical densities of the BCN phase (ρ (BaCo1/3Nb2/3O3)= 6.5 g/cm3, JCPDS card No. 46–0997). The closed porosity was calculated from the

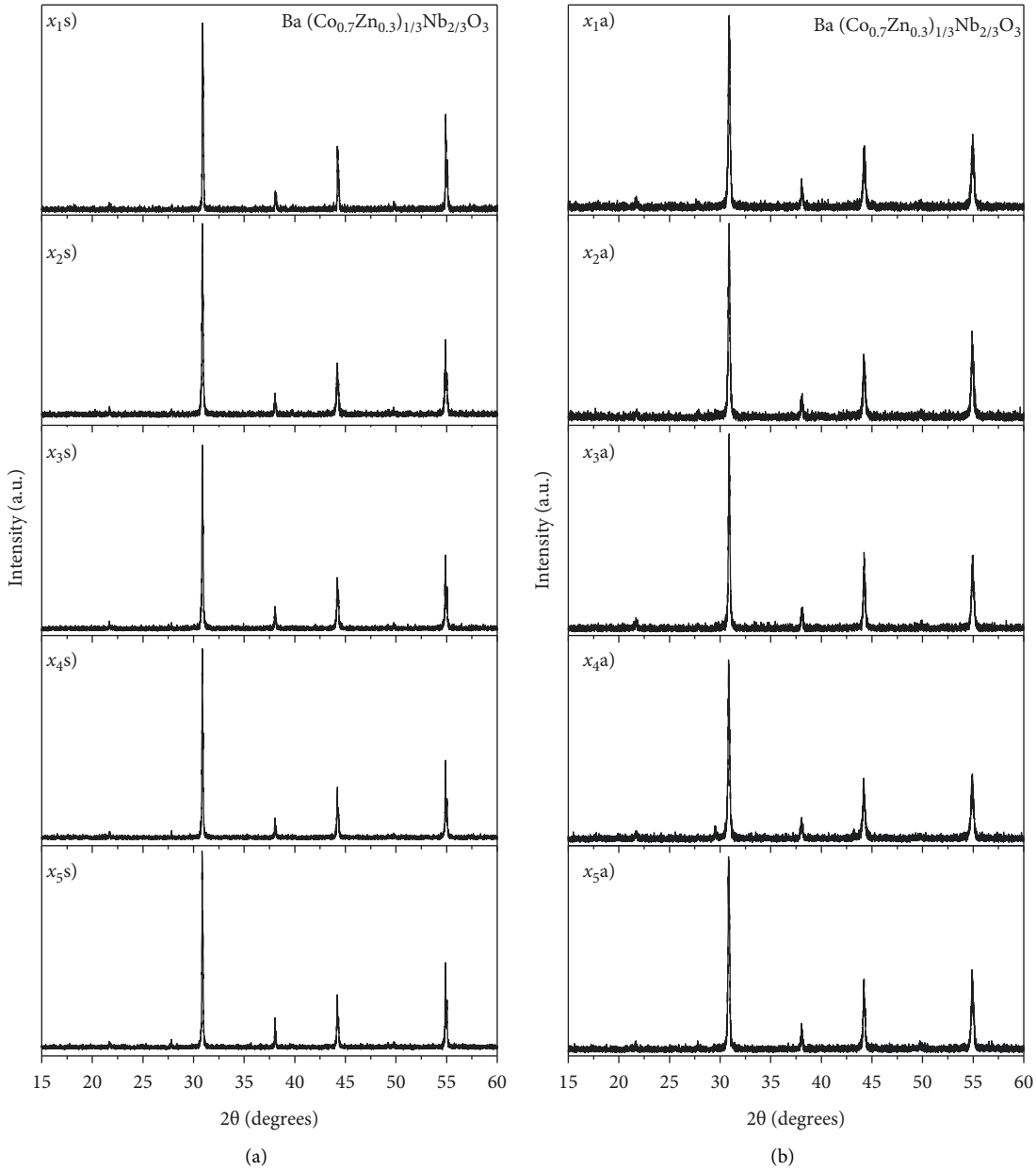

Figure 3: X-ray diffraction pattern for bulk BCZN ceramics: (a) BCZN sintered ceramics recorded for different thermal cycles and (b) BCZN annealed ceramics at 1300°C for 30 h.

skeleton (He pycnometry) and theoretical density, and these latter porosities (total and closed) are used to calculate the open porosity. The linear shrinkage was calculated by using the ΔL/L0 ratio (where ΔL is the change in length of the annealed ceramic, and L0 is the initial length of the specimen). As shown in Table 2, regardless of the heat thermal process, all samples have a large relative density (skeletal) of about 6.3 g/cm3, that is, >96% of the theoretical density (T. D.) (see Figure 6). Therefore, all specimens exhibit low total porosity ranging from 3 to 4.5%. The closed porosity was in the range 2–3%, and the open porosity was about 1%. This lower porosity can be explained by the high density of the BCZN ceramic that is very near to theoretical density. Higher values of shrinkage of about 16% are observed for all the annealed ceramics. This is in good agreement with the skeletal density which is ~6.3 g/cm3.

3.2. Microwave Dielectric Properties. The microwave dielectric properties measured at about 6 GHz of the Ba (Co0.7Zn0.3)1/3Nb2/3O3 (BCZN) ceramics were investigated for all specimens after the RRS technique under air at 1450°C for different thermal cycles and after annealing process at 1300°C for 30 hours in the air. Figure 6 shows the relative density and quality factor (QF) as a function of sintering process time for BCZN ceramics. The results of the dielectric characteristic measurements of the annealed Ba (Co0.7Zn0.3) 1/3Nb2/3O3 specimens are summarized

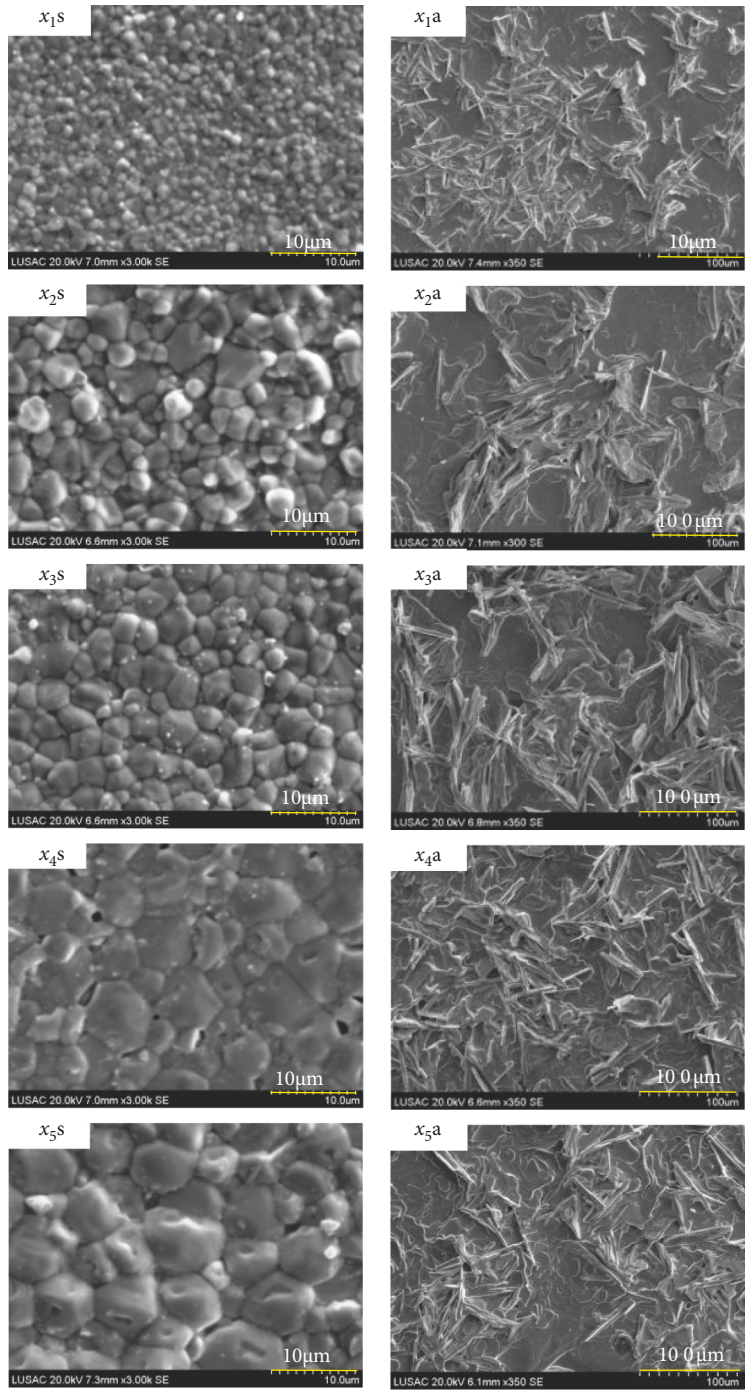

Figure 4: SEM images of the surface of BCZN ceramics. (a) On the surface after sintering. (b) On the surface after annealing.

Table 3. It is interesting to remark on Table 3 that regardless of thermal cycle conditions used of the RRS technique, the sintered BCZN ceramics exhibit low values of QF. The QF values measured in the present work increase with the sintering process time, from 31 830 (x1s-sample) to 52 799 GHz (x5s-sample) together with the increase of the grain size of ceramics (see Figure 4(a)). It should be noted that the presence of these secondary phases on the specimen surface (BCZN) seems to have no effect on the dielectric properties [3]. This is due to good microwave dielectric properties of the Ba5Nb4O15 and Ba8 (Co, Zn) 1Nb6O24 phases [15, 17, 18]. Vanderah et al. reported that the Ba5Nb4O15 is a cation-deficient perovskite and that the general formula can be written as follows: AnBn-1O3n [19]. Densified Ba5Nb4O15 ceramics exhibit the good microwave dielectric properties of $\varepsilon r = 39.2$, QF= 27 200 GHz, and $\tau f = 72$ ppm C^{-1} [18]. On the other hand, Solomon et al. reported that Ba8ZnNb6O24 has a quality factor (QF) equal to 10 890 GHz

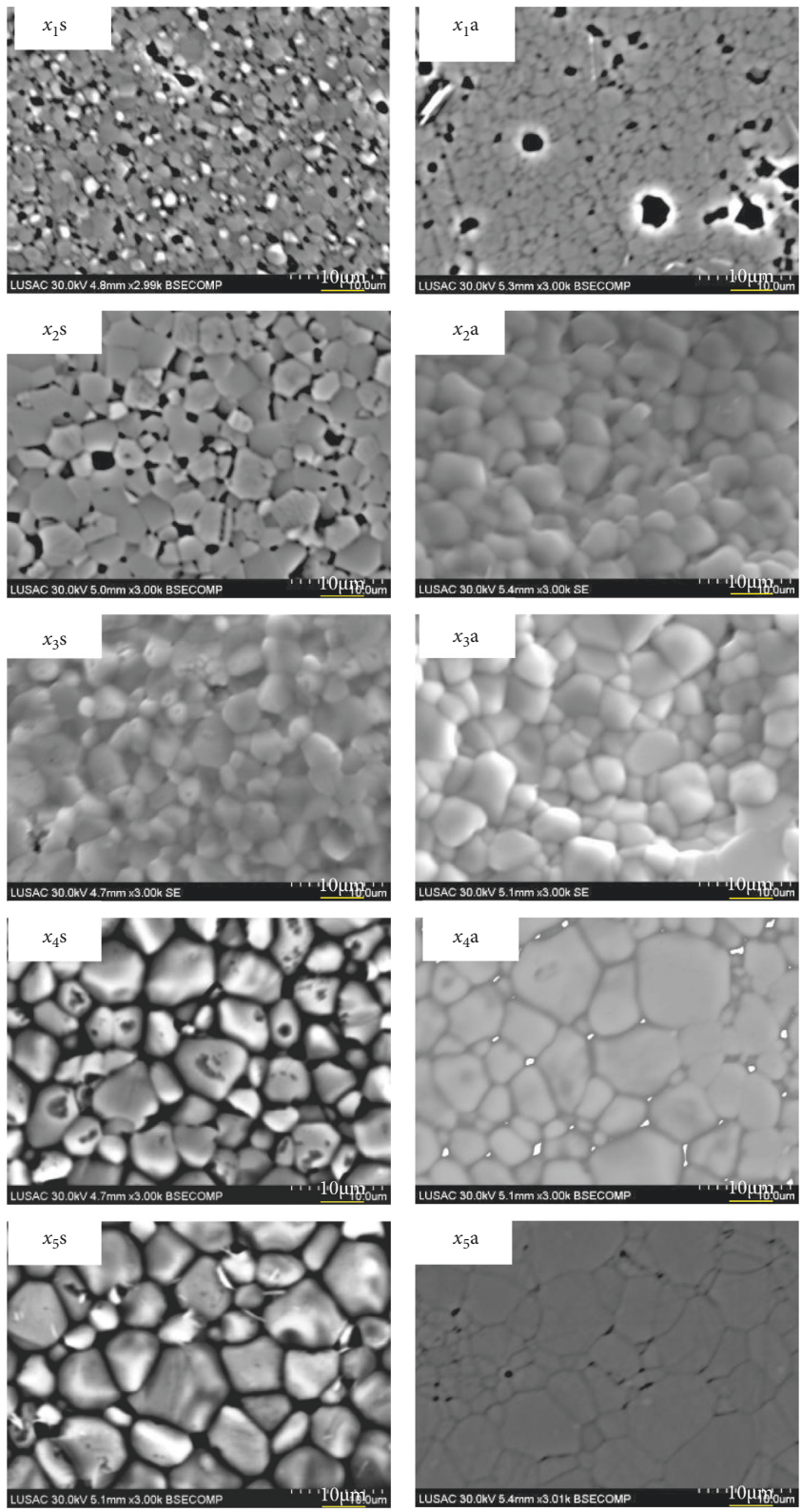

(a) (b)

Figure 5: SEM images of BCZN bulk ceramics. (a) BCZN sintered ceramics for different thermal cycles and (b) BCZN annealed ceramics at 1300°C for 30 h.

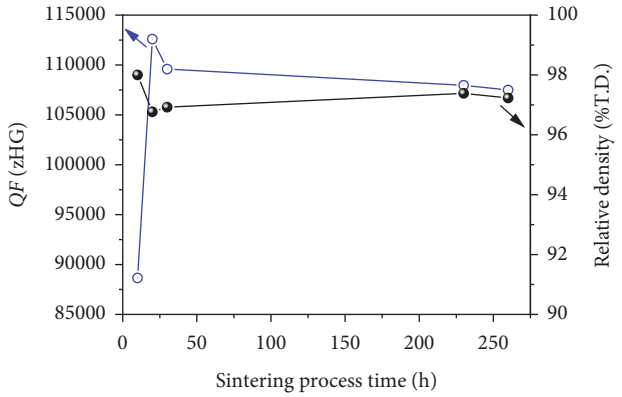

Figure 6: The relative density and QF of BCZN ceramics versus the thermal process time. T.D.: theoretical density.

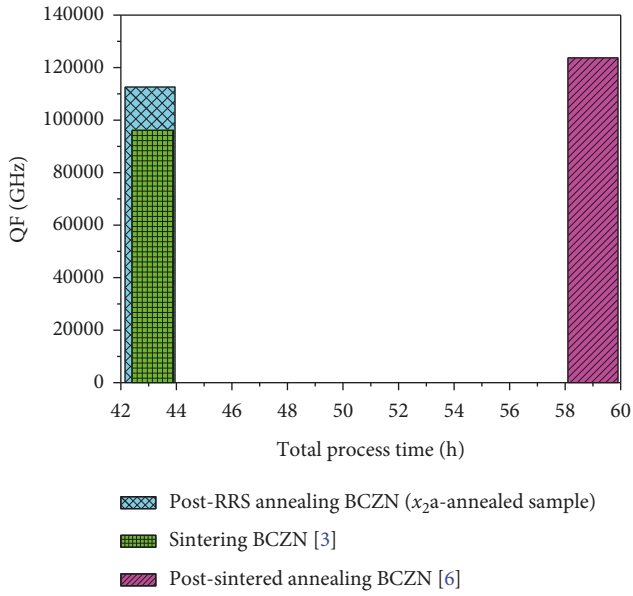

Figure 7: QF values of BCZN ceramics versus the thermal process time for three processes (post-RRS annealing, sintering, and postsintered annealing).

at 3.96 GHz, a relative dielectric constant $\varepsilon r = 36.26$, and a temperature coefficient of resonant frequency $\tau f = 49.9$ ppm C^{-1} [15]. The thermal annealing process greatly improves the QF values: high QF values close to 110 000 GHz were obtained for all annealed ceramics, except for the x1a-sample which shows a value of 88 653 GHz. On the other hand, if we consider the total treatment time including the RRS technique and annealing process times, the QF values measured in annealed pellets increase significantly with total time to reach a maximum (x2a-sample) followed by stabilization of the QF values (see Figure 6). Furthermore, as shown in Table 3, the maximum QF value of 112 598 GHz is observed of the x2a-annealed sample. As a matter of fact, we have already shown that the improvement of the annealing QFs are due to the degree of 1: 2 cation ordering within the BCZN crystal, which is taking place during the annealing process [6]. The high dielectric constant εr of ~34.5 and a temperature coefficient of the resonant frequency τf of ~0 ppm C^{-1} were obtained in all annealed ceramics. It is important to note that the sintered and annealed pellets exhibit the same values of εr and τf. From these results in this study, it can be concluded that the effect of the grain size and porosity may be small in the improvement of QFs of BCZN ceramics. Moreover, it is noticeable that the 1: 2 cation ordering into the BCZN perovskite structure plays a key role in improving the factor quality.

In order to highlight the advantages of the RRS technique, a comparison between QF values of the RRS sample with those obtained by other processes (given in references [3, 6]) is carried out. The QF values of BCZN ceramics obtained by the RRS technique, sintering, and postsintered annealing are plotted in Figure 7. It is interesting to remark on Figure 7 that the high QF-value of 112 598 GHz is observed of the post-RRS annealed BCZN sample (x2a-annealed sample) corresponding to 43h05 of total process time. Moreover, the postsintered annealing process exhibits the highest QF value (123 700 GHz [6]) for which a longer processing time is required (59h00). The sintering process with a total time of 43h15 permit to have a QF of 96 132. This comparison shows a compromise to be kept between a high QF and a shorter processing time.

4. Conclusion

The influence of the heat treatment by using the RRS technique on the structural and microstructural characteristics of the Ba (Co0.7Zn0.3) 1/3Nb2/3O3 ceramics was investigated by combining XRD and SEM analyses. The relationship between structural/microstructural characteristics and microwave dielectric proprieties of BCZN ceramics was explored. Dense dielectric BCZN ceramic materials can be achieved in a shorter sintering time by using the RRS technique. Thus, the rapid-rate sintering technique permits to produce pure BCZN ceramic materials on both the surface and in bulk by avoiding the secondary phase formation on the BCZN ceramic surface. Ba5Nb4O15 and Ba8 (Co, Zn) 1Nb6O24 are secondary surface phases, and it was detected only when the BCZN sample was annealed at 1300°C for 30 hours, which is different in the case of conventional sintering treatment. The Ba (Co0.7Zn0.3) 1/3Nb2/3O3 ceramics exhibit the morphologies of round shaped grains, and the Ba8 (Co, Zn) 1Nb6O24 phase highlights needle-shaped grains.

The microwave dielectric properties are not affected by the rapid-rate sintering process (RRS); however, they depend sensitively by the second heat treatment (annealing process). The high QF value of 112 101 GHz was observed for the BCZN sample sintered at 1450°C under air with rapid-rate sintering (insertion/extraction times of 5/5 minutes) and with a short holding time of 10 min followed by a longer annealing process time at 1300°C for 30 h in the air.

Finally, and in comparison to the conventional sintering processing, large time savings of 16.25 hours were recorded by using the RRS technique to have cleaner BCZN ceramic materials with the same high microwave dielectric properties ($\varepsilon r = 34.5$, QF= 112 598 GHz, and $\tau f = 0$ ppm C^{-1}).

Data Availability

The figures, images, tables, and text data used to support the findings of this study are available from the corresponding author upon request.

Conflicts of Interest

The authors declare that they have no conflicts of interest.

Acknowledgments

This work was supported by the French National Research Agency (ANR) [cheap components].

References

[1] R. I. Scott, M. Thomas, and C. Hampson, "Development of low cost, high performance Ba(Zn1/3Nb2/3O3) based materials for microwave resonator applications," *Journal of the European Ceramic Society*, vol. 23, no. 14, pp. 2467–2471, 2003.

[2] F. Azough, R. Freer, D. Iddles, T. Shimada, and B. Schaffer, "The effect of cation ordering and domain boundaries on low loss Ba(BI1/3BII2/3)O3 perovskite dielectrics revealed by high-angle annulardark-field scanning transmission electron microscopy (HAADF STEM)," *Journal of the European Ceramic Society*, vol. 34, no. 10, pp. 2285–2297, 2014.

[3] B. Itaalit, M. Mouyane, J. Bernard, J.-M. Reboul, and D. Houivet, "Improvement of microwave dielectric properties of Ba(Co0.7Zn0.3)1/3Nb2/3O3 ceramics prepared by solid-state reaction," *Ceramics International*, vol. 14, pp. 1937–1942, 2015.

[4] K. Endo, K. Fujimoto, and K. Murakawa, "Dielectric properties of ceramics in Ba (Co1/3 Nb2/3)O3-Ba(Zn1/3Nb2/3)O3 solid solution," *Journal of the American Ceramic Society*, vol. 70, no. 9, pp. C-215–C-218, 1987, C-215-C-218.

[5] C.-W. Ahn, H.-J. Jang, S. Nahm, H.-M. Park, and H.-J. Lee, "Effects of microstructure on the microwave dielectric properties of Ba(Co1/3Nb2/3)O3 and (1−x)Ba(Co1/3Nb2/3)O3–xBa(Zn1/3Nb2/3)O3 ceramics," *Journal of the European Ceramic Society*, vol. 23, no. 14, pp. 2473–2478, 2003.

[6] B. Itaalit, M. Mouyane, J. Bernard, M. Womes, and D. Houivet, "Effect of post-annealing on the microstructure and microwave dielectric properties of Ba(Co0.7Zn0.3)1/3Nb2/3O3 ceramics," *Applied Sciences*, vol. 6, no. 1, p. 2, 2015.

[7] F. Azough, C. Leach, and R. Freer, "Effect of CeO2 on the sintering behaviour, cation order and properties of Ba3Co0.7Zn0.3Nb2O9 ceramics," *Journal of the European Ceramic Society*, vol. 26, no. 10-11, pp. 1883–1887, 2006.

[8] A. Mergen and E. Korkmaz, "Effect of In, Ce and Bi dopings on sintering and dielectric properties of Ba(Zn1/3Nb2/3)O3 ceramics," *Journal of the European Ceramic Society*, vol. 31, no. 14, pp. 2649–2655, 2011.

[9] Y. Zhang, X. Zhou, X. Yang, C. Sun, F. Yang, and H. Chen, "Effects of Y2O3/CeO2 co-doping on microwave dielectric properties of Ba(Co0.6Zn38)1/3Nb2/3O3 ceramics," *Journal of Alloys and Compounds*, vol. 679, pp. 247–253, 2016.

[10] C. Genuist and F. M. Haussonne, "Sintering of BaTiO3: dilatometric analysis of diffusion models and microstructure control," *Ceramics International*, vol. 14, no. 3, pp. 169–179, 1988.

[11] A. Morell and A. Hermosin, "Fast sintering of soft Mn-Zn and Ni-Zn ferrite pot cores," *American Ceramic Society Bulletin*, vol. 59, no. 6, pp. 626–629, 1980.

[12] A. Morell, "Magnetic properties and microstructure of coprecipitated Ni-Zn ferrites sintered by hot-pressing, conventional and fast-firing," *Journal of Magnetism and Magnetic Materials*, vol. 31-34, pp. 997-998, 1983.

[13] J. Wang, K. Ning, J. Zhang et al., "Rapid rate sintering of yttria transparent ceramics," *Journal of the American Ceramic Society*, vol. 99, no. 6, pp. 1935–1942, 2016.

[14] J. H. Lee, B.-C. Kim, J. J. Kim, T. Ikegami, and T. Ikegami, "Rapid rate sintering of nanocrystalline indium tin oxide ceramics: particle size effect," *Materials Letters*, vol. 52, no. 1-2, pp. 114–119, 2002.

[15] S. Solomon, M. K. Suresh, J. K. Thomas, V. S. Prasad, and P. Wariar, "Synthesis, structural analysis and dielectric properties of Ba8(Mg1-xZnx)Nb6O24 hexagonal perovskites," *Ceramics International*, vol. 38, no. 8, pp. 6487–6494, 2012.

[16] F. Azough, C. Leach, and R. Freer, "Effect of nonstoichiometry on the structure and microwave dielectric properties of Ba(Co1/3Nb2/3)O3 ceramics," *Journal of the European Ceramic Society*, vol. 26, no. 14, pp. 2877–2884, 2006.

[17] J. R. Kim, D. W. Kim, H. S. Jung, and K. S. Hong, "Low-temperature sintering and microwave dielectric properties of Ba5Nb4O15 with ZnB2O4 glass," *Journal of the European Ceramic Society*, vol. 26, no. 10-11, pp. 2105–2109, 2006.

[18] H. Zhou, X. Chen, L. Fang, C. Hu, and H. Wang, "Microwave dielectric properties of Ba5Nb4O15 ceramic by molten salt method," *Journal of Materials Science: Materials in Electronics*, vol. 21, no. 9, pp. 939–942, 2010.

[19] T. A. Vanderah, R. S. Roth, T. Siegrist, W. Febo, J. M. Loezos, and W. Wong-Ng, "Subsolidus phase equilibria and crystal chemistry in the system BaO-TiO2-Ta2O5," *Solid State Sciences*, vol. 5, no. 1, pp. 149–164, 2003.